IBRACON Structures and Materials Journal
Revista IBRACON de Estruturas e Materiais
ISSN 1983-4195 ismj.org

ORIGINAL ARTICLE

Applicability of the 500°C isotherm method in determining the strength of reinforced concrete beams after fire

Aplicabilidade do método dos 500°C na determinação da resistência de vigas em concreto armado após incêndio

Leonardo Medeiros da Costa[a]
José Jeferson do Rêgo Silva[b]
Tiago Ancelmo de Carvalho Pires de Oliveira[b]
Dayse Cavalcanti de Lemos Duarte[c]

[a]Universidade Estadual da Paraíba – UEPB, Departamento de Engenharia Civil, Araruna, PB, Brasil
[b]Universidade Federal de Pernambuco – UFPE, Departamento de Engenharia Civil, Recife, PE, Brasil
[c]Universidade Federal de Pernambuco – UFPE, Departamento de Engenharia Mecânica, Recife, PE, Brasil

Received 03 March 2021
Accepted 02 August 2021

Abstract: A procedure to estimate the residual bending moment and the shear load capacity after fire in reinforced concrete beams was evaluated. The calculation method is based on the 500ºC Isotherm Method, adopting the reduction coefficients proposed by Van Coile et al. (2014) for the steel yield strength. The proposed method validation was done from experimental results of 62 reinforced concrete beams available in the literature. It was possible to observe a good approximation of the analytical method with the experimental data. For the bending moment an average ratio M_r^{ana} / M_r^{exp} of 1.04 and standard deviation of 0.15 was found. For the shear force an average ratio V_r^{ana} / V_r^{exp} of 0.85 and standard deviation of 0.23 was found.

Keywords: residual strength, shear, bending moment, after fire.

Resumo: Um procedimento para estimar a capacidade residual após incêndio para o momento fletor e o cisalhamento em vigas de concreto armado foi avaliado. O método de cálculo é baseado no Método das Isotermas dos 500ºC, adotando os coeficientes de redução propostos por Van Coile et al. (2014) para resistência ao escoamento do aço. A validação foi feita com resultados experimentais de 62 vigas disponíveis na literatura e foi possível observar uma boa aproximação com os dados experimentais, apresentando para o momento fletor uma relação média M_r^{ana} / M_r^{exp} de 1.04 e desvio padrão médio de 0.15, e para o esforço cortante uma relação média V_r^{ana} / V_r^{exp} de 0.85 e desvio padrão médio de 0.23.

Palavras-chave: resistência residual, cisalhamento, momento fletor, após incêndio.

How to cite: L. M. Costa, J. J. R. Silva, T. A. C. P. Oliveira, and D. C. L. Duarte, "Applicability of the 500°C isotherm method in determining the strength of reinforced concrete beams after fire", *Rev. IBRACON Estrut. Mater.*, vol. 15, no. 2, e15202, 2022, https://doi.org/10.1590/S1983-41952022000200002

1 INTRODUCTION

It is known that fires can cause serious damage to reinforced concrete structural elements. In particular, the beams and slabs are located at the top of the building and are more prone to fire damage, as highlighted by Yang et al. [1]. In the absence of a failure during the fire, measuring the level of damage caused after a fire is essential in deciding either to release the use, to repair or to demolish the structure.

Corresponding author: Leonardo Medeiros da Costa. E-mail: leonardom.costa@yahoo.com.br
Financial support: None.
Conflict of interest: Nothing to declare.

Determining the residual capacity of reinforced concrete (RC) beams involves understanding the effects of temperature on concrete and steel. Concrete has a good fire performance due to its low thermal conductivity and high thermal capacity but presents loss on the residual strength depending on the severity of the fire [2], [3]. After fire temperatures between 500 and 600ºC, the steel recovers its strength to room temperatures, as indicated by Neves et al. [4] and Van Coile et al. [5], respectively.

Molkens et al. [6] note that for most fires in buildings with concrete structure, the structural elements do not collapse during the fire exposure. However, after fire a change in the critical failure mode can occur. Thanaraj et al. [7] reported experimental series where the elements started to fail due to shear. This same behavior is observed by Diab [8] reporting that shear failure can be critical on reinforced concrete beams after fire, being an aggravating factor that this is sudden type of rupture. This tendency to shear failure in RC beams after fire occurs in elements with low compressive strength concrete, decreasing the shear capacity of the elements because concrete is an important part of shear strength. Other factors such as w/c ratio, density and reinforcement percentage are also an influence on the failure mode [7].

In the ABNT NBR 15200 [9], Eurocode 1 1-2 [10] and Eurocode 2 1-2 [11] standards, there is no clear recommendation on the assessment of residual load capacity in reinforced concrete elements after a fire situation. In the literature, some authors have proposed analytical formulations to determine the residual strength of reinforced concrete beams and the most relevant references in this regard are here presented.

The residual strength after fire of other materials such as high-strength mortar, wood, and masonry is reported in the literature. Cülfik and Özturan [12] observed a significant loss on mortars residual strength for temperatures up to 600ºC and almost full strength loss for temperatures up to 900ºC. Sciarretta [13] numerically analyzed masonry walls after fire and found satisfactory results compared to experimental results available in the literature.

Hsu and Lin [14] proposed an approach based on the ACI 318 [15] considering the deformation compatibility to evaluating the residual load capacity of beams exposed to fire. It was observed that the reduction on the bending moment and shear force capacity are different: the shear capacity after fire is about 53.0% and 40.8% of the initial capacity, while the residual bending moment is about 65.13% and 52.83% of the initial capacity, when the beams are exposed to fire for 120 and 180 minutes, respectively.

Kodur et al. [16] presented a simplified approach for calculating residual flexural strength of reinforced concrete beams based on ACI 318 [17], applying the reduction factors for the strength of steel and concrete. The maximum temperature and duration of the fire were estimated through visual observations of the exposed concrete. As a result, the residual bending moment was conservative.

Bai and Wang [18] proposed a method based on the design at room temperature for the residual flexural strength of reinforced concrete beams after fire, considering reducing the concrete and reinforcement steel sections to compensate the damage caused by the fire. In a parametric study, they concluded that the initial strength of concrete and steel have few influences on the residual strength results. The percentual strength reduction after fire exposure is near for all the strength values analyzed.

Xu et al. [19]–[21] presented experimental studies analyzing the residual strength after fire to shear and the bending moment of reinforced concrete beams with rectangular and "T" sections. In Xu et al. [20] a study on estimating of the resistance after fire is presented based on the Chinese code [22], reducing the strengths of concrete and steel as a function of temperature.

Numerical simulations were developed by Kodur and Agrawal [23], Sun et al. [24] and Cai et al. [25], but refined analysis requires a high computational cost. As it is possible to observe in the available literature, few analytical models to estimate the residual strength of reinforced concrete beams after fire are formulated. Even more scarce is the analysis of post-fire shear capacity, as research is often conditioned to the verification of flexural strength.

The present paper aims to validate the application of a simplified procedure to estimate the bending moment and the shear capacity in reinforced concrete beams after fire. The method is based on the 500ºC Isotherm Method [11], adopting the reduction coefficients proposed by Van Coile et al. [5] to the yield strength of steel.

2 EXPERIMENTAL DATA

2.1 Post-fire moment capacity

A total of 22 beams tested experimentally were used to verify the method for determining the post-fire moment capacity and are available in the literature. The beams were heated on three faces, without load during the heating phase and tested post-fire with four-point bending, Figure 1. All beams failed in flexure. More details are present in Thanaraj et al. [7], Xu et al. [20] and Pereira et al. [26]. It is noteworthy to mention that only beams that lost strength after fire are included in the validation. RC beams under short-time heating and low peak temperatures tended to have no relevant loss of strength.

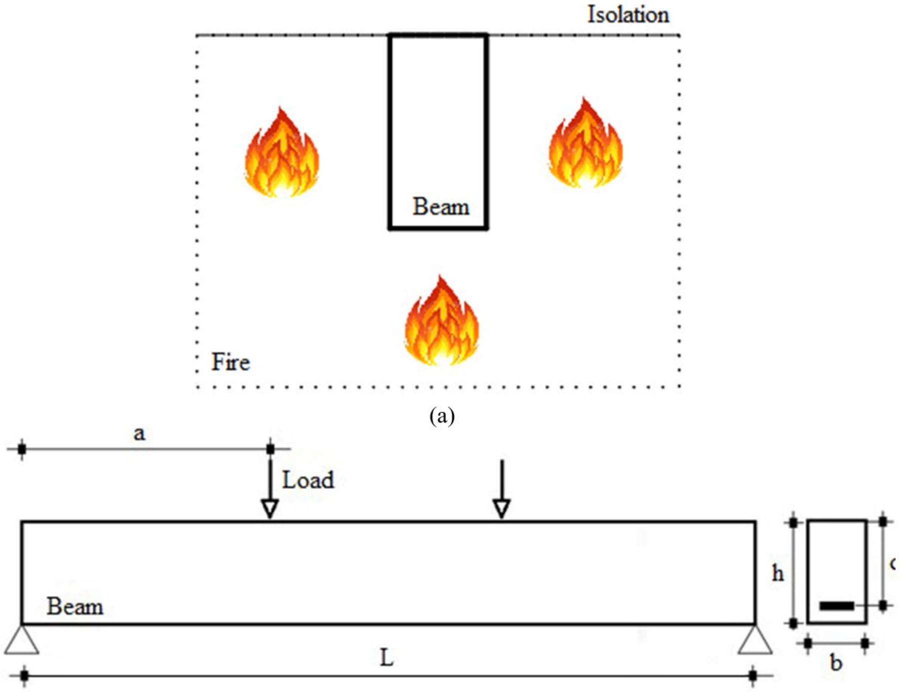

(b)

Figure 1. Tests (a) heating phase on cross section and (b) four-point bending after fire

The parameters considered in the beams were: cross section, concrete strength, time of exposure to fire, transverse reinforcement ratio (ρ_t), longitudinal reinforcement ratio (ρ_l) and shear span (ξ), see Table 1

Where: A_s: area of longitudinal reinforcement; A_{sw}: area of transverse reinforcement area; s: stirrups spacing

Table 1. Identification and characteristics of beams analyzed by bending

Ref.	**ID.**	**Cross Section**	**Fire curve**	**Time**	**f_c**	$\rho_l = \frac{A_s}{b \cdot h}$	$\rho_t = \frac{A_{sw}}{b \cdot s}$	$\xi = a / d$
-	**-**	**-**	**-**	**(min)**	**(MPa)**	**%**	**%**	**-**
[20]	L5	25x40	ISO 834	60	41.2	1.47%	0.27%	1.51
[20]	L6	25x40	ISO 834	60	41.2	1.47%	0.27%	1.71
[20]	L7	25x40	ISO 834	60	41.2	1.47%	0.27%	2.22
[20]	L9	25x40	ISO 834	120	41.2	1.47%	0.27%	3.31
[26]	REC15_210	12x20	NS	210	47.6	0.65%	0.79%	1.43
[26]	REC30_210	12x20	NS	210	47.6	0.65%	0.79%	1.57
[7]	M20-60	20x20	ISO 834	60	27.09	0.39%	0.62%	1.23
[7]	M20-120	20x20	ISO 834	120	27.09	0.39%	0.62%	1.23
[7]	M20-180	20x20	ISO 834	180	27.09	0.39%	0.62%	1.23
[7]	M20-240	20x20	ISO 834	240	27.09	0.39%	0.62%	1.23
[7]	M30-60	20x20	ISO 834	60	37.8	0.39%	0.62%	1.23

Table 1. Continued…

Ref.	ID.	Cross Section	Fire curve	Time	f_c	$\rho_l = \frac{A_s}{b \cdot h}$	$\rho_t = \frac{A_{sw}}{b \cdot s}$	$\xi = a / d$
-	-	-	-	(min)	(MPa)	%	%	-
[7]	M30-120	20x20	ISO 834	120	37.8	0.39%	0.62%	1.23
[7]	M30-180	20x20	ISO 834	180	37.8	0.39%	0.62%	1.23
[7]	M30-240	20x20	ISO 834	240	37.8	0.39%	0.62%	1.23
[7]	M40-60	20x20	ISO 834	60	47.31	0.39%	0.62%	1.23
[7]	M40-120	20x20	ISO 834	120	47.31	0.39%	0.62%	1.23
[7]	M40-180	20x20	ISO 834	180	47.31	0.39%	0.62%	1.23
[7]	M40-240	20x20	ISO 834	240	47.31	0.39%	0.62%	1.23
[7]	M50-60	20x20	ISO 834	60	56.67	0.39%	0.62%	1.23
[7]	M50-120	20x20	ISO 834	120	56.67	0.39%	0.62%	1.23
[7]	M50-180	20x20	ISO 834	180	56.67	0.39%	0.62%	1.23
[7]	M50-240	20x20	ISO 834	240	56.67	0.39%	0.62%	1.23

NS – Non-Standard

The influence of the ratio (a / d) on the post-fire moment capacity in the tested beams was not identified. The procedure was also shown to be applicable to non-standard fire curves. As expected, longer times of exposure to fire resulted in greater resistance reductions, especially for concretes of lower resistance. The compressive strength also influenced the failure mode.

2.2 Post-fire shear capacity

A total of 40 beams tested experimentally with results available in the literature were used in the validation of the procedure to estimate the post-fire shear capacity of reinforced concrete beams. The beams were heated on three faces, without load during the heating phase and tested post-fire with four-point bending. The identification and characteristics of the beams are shown in Table 2.

Table 2. Identification and characteristics of the beams analyzed to shear

Ref.	ID.	Cross Section	Fire curve	Time	f_c	$\rho_l = \frac{A_s}{b \cdot h}$	$\rho_t = \frac{A_{sw}}{b \cdot s}$	ξ=a/d	a / L
-	-	(cm)	-	(min)	(MPa)	(%)	(%)	-	-
[27]	V120	20x30	ISO 834	120	17.1	0.75%	0.14%	4.4	0.25
[27]	V60	20x30	ISO 834	60	17.1	0.75%	0.14%	4.4	0.25
[27]	V90	20x30	ISO 834	90	17.1	0.75%	0.14%	4.4	0.25
[14]	test nº17	30x45	ASTM E119	60	34.7	2.53%	0.00%	1.5	0.36
[14]	test nº18	30x45	ASTM E119	180	34.7	2.53%	0.00%	1.5	0.36
[14]	test nº2	20x30	ASTM E119	60	34.7	1.90%	0.00%	1.5	0.33
[14]	test nº27	20x30	ASTM E119	60	60.5	1.90%	0.00%	1.5	0.33
[14]	test nº28	20x30	ASTM E119	180	62.5	1.90%	0.00%	1.5	0.33

Table 2. Continued…

Ref.	ID.	Cross Section	Fire curve	Time	fc	$\rho_l = \frac{A_s}{b \cdot h}$	$\rho_t = \frac{A_{sw}}{b \cdot s}$	ξ=a/d	a / L
-	-	(cm)	-	(min)	(MPa)	(%)	(%)	-	-
[14]	test nº3	20x30	ASTM E119	180	34.7	1.90%	0.00%	1.5	0.33
[14]	test nº32	20x30	ASTM E119	60	65.2	3.80%	0.00%	1.5	0.32
[14]	test nº33	20x30	ASTM E119	180	66.5	3.80%	0.00%	1.5	0.32
[14]	test nº8	20x30	ASTM E119	60	35.8	3.80%	0.00%	1.5	0.32
[14]	test nº9	20x30	ASTM E119	180	35.8	3.80%	0.00%	1.5	0.32
[14]	test nº14	20x30	ASTM E119	60	34.7	1.90%	0.98%	1.5	0.33
[14]	test nº15	20x30	ASTM E119	180	34.7	1.90%	0.98%	1.5	0.33
[14]	test nº23	30x45	ASTM E119	180	34.7	2.53%	0.98%	1.5	0.36
[14]	test nº11	20x30	ASTM E119	60	35.8	3.80%	0.00%	4.0	0.41
[14]	test nº12	20x30	ASTM E119	180	35.8	3.80%	0.00%	4.0	0.41
[14]	test nº20	30x45	ASTM E119	60	35.8	5.47%	0.00%	4.0	0.44
[14]	test nº21	30x45	ASTM E119	180	35.8	5.47%	0.00%	4.0	0.44
[14]	test nº30	20x30	ASTM E119	60	71.6	1.90%	0.00%	4.0	0.42
[14]	test nº35	20x30	ASTM E119	60	65.7	3.80%	0.00%	4.0	0.41
[14]	test nº25	30x45	ASTM E119	180	35.8	5.47%	0.52%	4.0	0.44
[20]	L4	25x40	ISO 834	60	41.2	1.47%	0.00%	2.2	0.36
[21]	L4	20x30	ISO 834	60	51.5	3.27%	0.17%	2.7	0.50
[28]	B5-2.1-f120	25x40	ISO 834	120	31.6	1.96%	0.00%	2.1	0.21
[28]	B5-2.1-f60	25x40	ISO 834	60	31.6	1.96%	0.00%	2.1	0.21
[28]	B5-2.1-f90	25x40	ISO 834	90	31.6	1.96%	0.00%	2.1	0.21
[28]	B6-2.1-f90	25x40	ISO 834	90	31.6	1.61%	0.00%	2.1	0.21
[28]	B7-2.1-f90	25x40	ISO 834	90	31.6	1.47%	0.00%	2.1	0.21
[28]	B4-2.1-f90	25x40	ISO 834	90	31.6	1.96%	0.20%	2.1	0.21
[28]	B1-2.1-f120	25x40	ISO 834	120	31.6	1.96%	0.27%	2.1	0.21
[28]	B1-2.1-f60	25x40	ISO 834	60	31.6	1.96%	0.27%	2.1	0.21
[28]	B1-2.1-f90	25x40	ISO 834	90	31.6	1.96%	0.27%	2.1	0.21
[28]	B2-2.1-f90	25x40	ISO 834	90	31.6	1.61%	0.27%	2.1	0.21
[28]	B3-2.1-f90	25x40	ISO 834	90	31.6	1.47%	0.27%	2.1	0.21
[28]	B5-2.6-f90	25x40	ISO 834	90	31.6	1.96%	0.00%	2.6	0.26
[28]	B1-2.6-f90	25x40	ISO 834	90	31.6	1.96%	0.27%	2.6	0.26
[28]	B5-3.3-f90	25x40	ISO 834	90	31.6	1.96%	0.00%	3.3	0.32
[28]	B1-3.3-f90	25x40	ISO 834	90	31.6	1.96%	0.27%	3.3	0.32

* ρ_t =0.00%: no stirrups

A relevant parameter is the ratio (a/d) that can modify the shear failure mode in reinforced concrete beams, as highlighted by Nakamura et al. [29]. Plasencia et al. [30] state that the failure of beams with ratio ($a/d<2$) was due to the rupture of the compression strut. This behavior was also observed in the post-fire shear capacity based on the experimental data presented, where the residual strength was influenced by the distance of the load applied to the support (a), effective height (d) and free span of the beam (L).

It is pertinent to observe that the formulations consider the shear span (ξ=a/d) and the ration (a / L) in the expressions to contemplate the "arc effect" that is promoted by the distance between the applied load and the support. It is also observed that the presence of stirrups changes the behavior of reinforced concrete beams, the calculation method being different for beams with or without transverse reinforcement.

3 PROPOSED PROCEDURE

The 500°C Isotherm method is applied to estimate the behaviour in fire situation and not to estimate the residual load bearing capacity of RC beams. The purpose of this paper is to extrapolate and verify its applicability in post fire situation.

The simplified method proved to be applicable to estimate the residual strength of RC beams independent of two important phenomena of concrete: (1) strength of concrete preheated to high temperature is after cooling (residual strength) lower than the strength at high temperature [31] and (2) concrete exposed to simultaneous action of high temperature and compressive stresses loses its strength much slower than concrete heated only (without compression) [32].

Figure 2 shows a flowchart for determining the residual strength of RC beams.

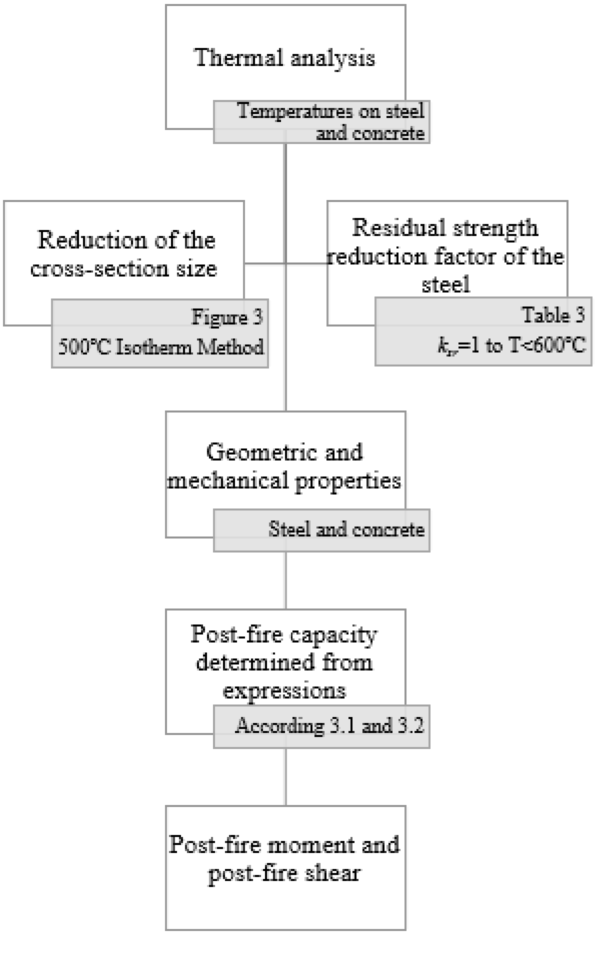

Figure 2. Procedure for determining residual strength

Thermal analyses are conducted first to obtain the temperature evolution in the cross section determined by FEM, through ABAQUS software, with 2D elements of 4 nodes (DC2D4) and 10x10mm mesh. The model accounts for the properties changes with the increase in temperature, considering the variation in conductivity and specific heat of the concrete (1.5% humidity) according to NBR15200 [9], as well as the emissivity of 0.7 and the heat transfer coefficient per convection of 25W/m²ºC.

The residual strength for the concrete was determined according to the 500ºC Isotherm Method [11]. In Figure 3, it is possible to identify the variables for a beam with three faces exposed to fire, where b_{fi} : it is the reduced width of the beam after fire (cm); d_{fi} : is the effective height of the beam after fire (cm); d_{500} : depth of the 500ºC isotherm (cm).

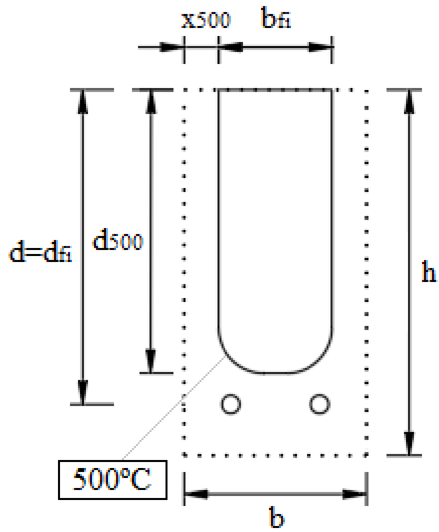

Figure 3. 500ºC Isotherm. (Source: Adapted [11])

Steel reinforcement bars have reduced strength using reduction factors (k_{sr}) proposed in Van Coile et al. [5] determined by a stochastic model based on experimental results, as shown in Table 3.

Table 3. Reduction factor for residual strength of steel

T (ºC)	20	50	100	200	400	550	600	700	850
k_{sr}	1	1	1	1	1	1	1	0.7	0.6

Source: Adapted from [5]

It is possible to notice that after fire, the steel reinforcement has a good capacity to recover its initial strength for temperatures up to 600ºC.

The longitudinal steel bars have the temperature measured on their axis, and the respective reducing coefficient is applied. The transverse steel bars had the reduction factor as a function of temperature at the point recommended in Eurocode 2 1-1 [33] to find point "P" at height $h_{c,ef}$ whose value is given by Equation 1:

$$h_{c,ef}=\min\left[2.5\left(h-d_{500}\right),\frac{\left(h-y_{\theta}\right)}{3},\frac{h}{2}\right] \tag{1}$$

Where: $h_{c,ef}$: is the height at point P from the beam bottom (cm); h : is the height of the beam (cm); y_{θ} : is the position of the neutral axis after a fire (cm).

The height ($h_{c,ef}$) refers to the region where the first shear cracks tend to appear. Other authors such as Xiang et al. [34] used the temperature at mean height of the stirrup and Diab [8] and Cai et al. [25] used the average over the height of the stirrup.

3.1 Post-fire moment capacity

The post-fire bending moment is determined from the 500ºC isotherm depth (d_{500}), width of the reduced section (b_{fi}) and the effective depth (d_{fi}) which remains the same as the cross section at room temperature. Figure 4 shows the balance of forces in the bending section.

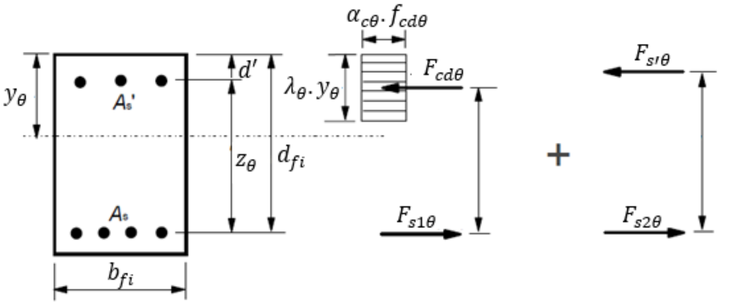

Figure 4. Equilibrium of forces in the bending section. (Source: Adapted [9])

Applying the balance of forces in the cross section, the concrete and steel forces can be calculated, in a procedure like the guidelines of NBR 6118 [35]. The coefficients α_c, γ_c e γ_s were adopted equal to 1 and λ_θ equal to 0.8.

3.2 **Post-fire shear capacity**

The estimated of the residual shear capacity after fire was based on the Model I proposed by the Brazilian standard [35] at room temperature that follows the model of classic truss with stirrups at 90º and compression struts at 45º.

Equations 2 to 7 presented below were adjusted based on the observation of the experimental behavior of the beams analyzed and include the relationships ($\xi = a/d$) and (a/L) in the formulation, discussed in section 2.

a) For beams without stirrups ($V_r^{ana} = V_{c\theta}$ *)*

$$V_{c\theta} = \frac{V_{Rd2}}{\xi}, \quad \xi \leq 2 \text{ The failure occurs in the compression strut of concrete with a value proportional to } \xi. \tag{2}$$

$V_{c0} \cdot \xi^{-a/L}$, $\quad 2 < \xi \leq 3.5$ The rupture occurs in the diagonal tension under the influence of a.

V_{c0}, $\quad \xi > 3.5$ Concrete is not influenced by ξ.

Where:

$$V_{c0} = 0.6 \cdot \frac{f_{ct}}{\gamma_c} \cdot b_{fi} \cdot d_{500} \tag{3}$$

$$V_{Rd2} = 0.27 \cdot \alpha_{v2} \cdot \frac{f_{ck}}{\gamma_c} \cdot b_{fi} \cdot d_{500} \tag{4}$$

$$\alpha_{v2} = 1 - \frac{f_{ck}}{250} \tag{5}$$

Where: V_r^{ana} : is the residual shear force; V_{Rd2} : is the shear force relative to the compression strut of concrete; V_{c0} : it is part resisted by complementary mechanisms.

b) For beams with stirrups ($V_r^{ana} = V_{R\theta}$ *)*

In the case of deep beams ($\xi \leq 2$) with shear reinforcement, the contribution of steel is reduced to smaller ξ. (Hayashikawa et al. [36] apud Nakamura et al. [29]).

$V_{R\theta} =$

$$\frac{V_{Rd2}}{\xi^{1+a/L}} + \frac{V_{sw}}{\xi},\ \xi \leq 2$$

Shear capacity provided by compressive strength of the concrete in the strut and the steel loses efficiency due to the proximity of the load applied with the support.

$$\frac{V_{c0}}{\xi^{1-a/L}} + V_{sw},\ 2 < \xi \leq 3.5 \tag{6}$$

Shear capacity provided by complementary mechanisms of concrete and steel has its effective contribution.

$$V_{c0} + V_{sw},\ \xi > 3.5$$

Concrete and steel are not influenced by ξ.

$$V_{sw} = \frac{A_{sw}}{s} \cdot k_{sr} \cdot \frac{f_{yk}}{\gamma_s} \cdot d_{500} \tag{7}$$

Where: V_{sw} : shear capacity provided by shear reinforcement. The coefficients γ_c and γ_s equal to 1.

4 RESULTS AND DISCUSSIONS

4.1 Post-fire moment capacity

Table 4 presents the results found for the residual bending moment and the relationships M_r^{ana} / M_r^{exp} between the analytical model and the experimental data.

Table 4. Analytical and experimental results for bending moment

Ref.	ID.	M_r^{exp}	M_{r1}^{ana}	M_{r1}^{ana} / M_r^{exp}
-	-	(kNm)	(kNm)	-
[20]	L5	196.0	210.9	1.08
[20]	L6	200.0	210.9	1.05
[20]	L7	197.0	210.9	1.07
[20]	L9	167.0	169.6	1.02
[26]	REC15_210	13.1	10.5	0.80
[26]	REC30_210	12.2	10.6	0.87
[7]	M20-60	9.2	11.8	1.28
[7]	M20-120	6.5	8.1	1.24

Table 4. Continued…

Ref.	**ID.**	$\mathbf{M_r^{exp}}$	$\mathbf{M_{r1}^{ana}}$	$\mathbf{M_{r1}^{ana} / M_r^{exp}}$
-	-	**(kNm)**	**(kNm)**	-
[7]	M20-180	5.6	6.9	1.23
[7]	M20-240	5.2	6.0	1.16
[7]	M30-60	11.3	12.0	1.06
[7]	M30-120	7.5	8.2	1.09
[7]	M30-180	5.8	7.0	1.21
[7]	M30-240	4.9	6.1	1.24
[7]	M40-60	13.6	12.2	0.89
[7]	M40-120	8.7	8.3	0.95
[7]	M40-180	7.0	7.1	1.01
[7]	M40-240	5.5	6.2	1.12
[7]	M50-60	15.8	12.3	0.78
[7]	M50-120	9.8	8.3	0.85
[7]	M50-180	8.0	7.1	0.89
[7]	M50-240	6.9	6.2	0.90
		Mean		*1.04*
		Standard Deviation		*0.15*
		Confidence Interval		*0.98-1.08*

The analytical-experimental results compiled in Table 4 result in an average ratio M_{r1}^{ana} / M_r^{exp} of 1.04 with a standard deviation of 0.15. The confidence interval was calculated with a 95% confidence level. Figure 5 plots the residual strength compared to the safety margin of ± 10%. Some samples of [7] showed a $M_{r1}^{ana} / M_r^{exp} > 1.2$ ratio, which may have been caused by the small cross-sectional dimensions of the beams and because exposure to the fire curve for a longer time.

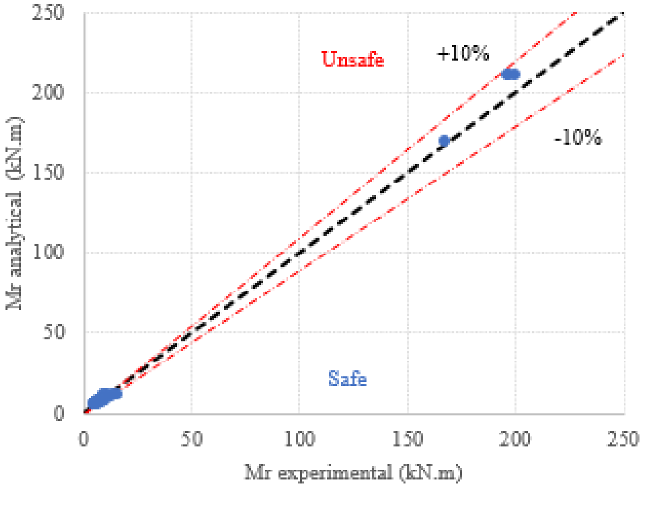

Figure 5. Post-fire moment capacity: analytical vs. experimental.

Figure 6 presents the results without the data from [20], which allows to analyze in more detail the group of beams that had a lower failure load and that consist of most of the data. The difference between the moments is justified by the large width dimension of the cross section (25x40cm) of the samples from [20].

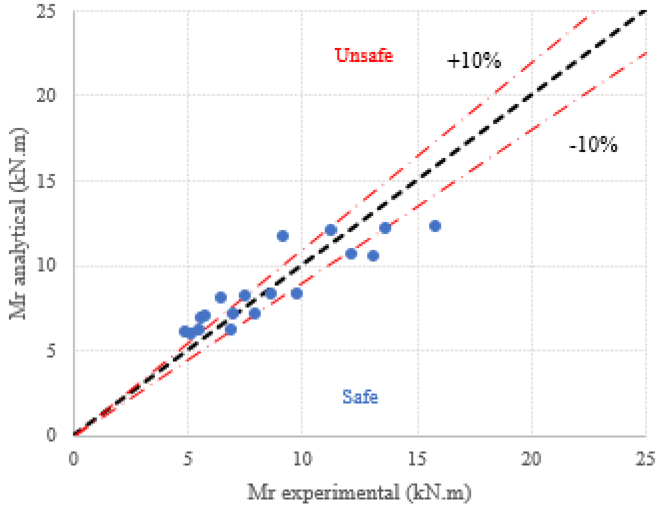

Figure 6. Post-fire moment capacity: analytical vs. experimental.

It is noteworthy to point that 14 beams showed a ratio M_{r1}^{ana} / M_r^{exp} greater than 1, with an average value of 1.13.

It is suggested, then, the proposition of a correction factor equal to 1.2 to match the model results, resulting in an average ratio M_{r2}^{ana} / M_r^{exp} of 0.86 with a standard deviation of 0.13. Figure 7 shows the results corrected by the coefficient.

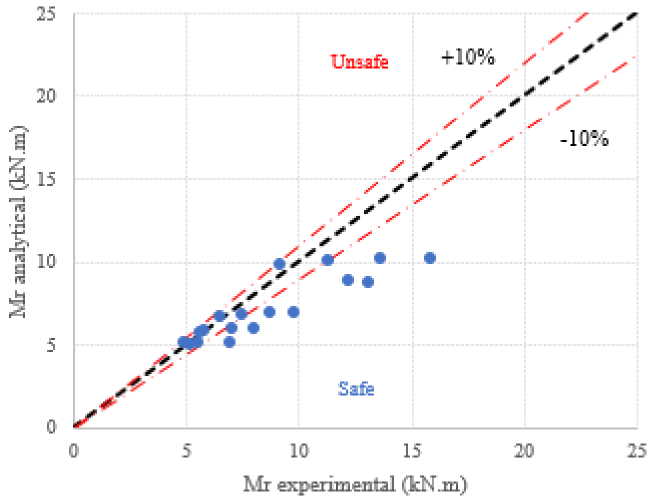

Figure 7. Post-fire moment capacity: analytical vs. experimental.

A total of 5 beams (22.72%) presented analytical results with ratio M_{r2}^{ana} / M_r^{exp} greater than 1, with an average value of 1.04 and coefficient of variation of 1.92%. No value was greater than the safety margin of 1.1. According to Coelho et al. [37], even though this may indicate that the results are less safe, they converge with the philosophy presented in the Eurocodes, where a prediction model must predict the phenomenon on its average, with the security of the model provided by safety factors. Therefore, the analytical procedure to measure the residual bending moment in reinforced concrete beams after fire, although simplified, can predict the bending resistance of beams after fire.

4.2 **Post-fire shear capacity**

Table 5 presents the results found for the shear by the analytical model compared to the experimental results through the ratio $V_{r1}^{ana} / V_{r}^{exp}$.

Table 5. Analytical and experimental results for shear force

Ref.	ID.	V_r^{exp}	V_{r1}^{ana}	V_{r1}^{ana} / V_r^{exp}
-	-	(kN)	(kN)	-
[24]	V120	47.4	45.9	0.97
[24]	V60	71.9	71.7	1.00
[24]	V90	61.9	55.0	0.89
[11]	test nº17	468.3	484.1	1.03
[11]	test nº18	279.0	387.3	1.39
[11]	test nº2	213.9	209.8	0.98
[11]	test nº27	337.5	321.9	0.95
[11]	test nº28	229.5	136.7	0.60
[11]	test nº3	188.8	87.1	0.46
[11]	test nº32	471.4	312.3	0.66
[11]	test nº33	246.5	140.5	0.57
[11]	test nº8	321.0	198.8	0.62
[11]	test nº9	220.7	89.4	0.41
[11]	test nº14	270.6	326.4	1.21
[11]	test nº15	243.1	139.7	0.57
[11]	test nº23	467.6	462.3	0.99
[11]	test nº11	89.2	49.3	0.55
[11]	test nº12	41.3	22.2	0.54
[11]	test nº20	211.9	123.2	0.58
[11]	test nº21	117.2	98.5	0.84
[11]	test nº30	89.8	75.8	0.84
[11]	test nº35	130.3	67.5	0.52
[11]	test nº25	311.1	195.6	0.63
[17]	L4	97.0	80.0	0.82
[18]	L4	147.0	50.4	0.34
[25]	B5-2.1-f120	60.0	65.1	1.08
[25]	B5-2.1-f60	80.0	76.6	0.96
[25]	B5-2.1-f90	71.3	72.8	1.02
[25]	B6-2.1-f90	79.0	72.8	0.92
[25]	B7-2.1-f90	80.0	72.8	0.91
[25]	B4-2.1-f90	132.5	114.7	0.87

Table 5. Continued…

Ref.	ID.	V_r^{exp}	V_{r1}^{ana}	V_{r1}^{ana} / V_r^{exp}
-	-	(kN)	(kN)	-
[25]	B1-2.1-f120	132.5	132.4	1.00
[25]	B1-2.1-f60	145.0	139.8	0.96
[25]	B1-2.1-f90	137.5	137.3	1.00
[25]	B2-2.1-f90	135.0	137.3	1.02
[25]	B3-2.1-f90	130.0	137.3	1.06
[25]	B5-2.6-f90	70.0	66.4	0.95
[25]	B1-2.6-f90	125.0	131.9	1.06
[25]	B5-3.3-f90	55.0	57.5	1.05
[25]	B1-3.3-f90	115.0	128.1	1.10
		Mean		0.85
		Standard deviation		0.23
		Confidence Interval		0.78-0.92

Figure 8 presents the results found experimentally and analytically for all the beams analyzed.

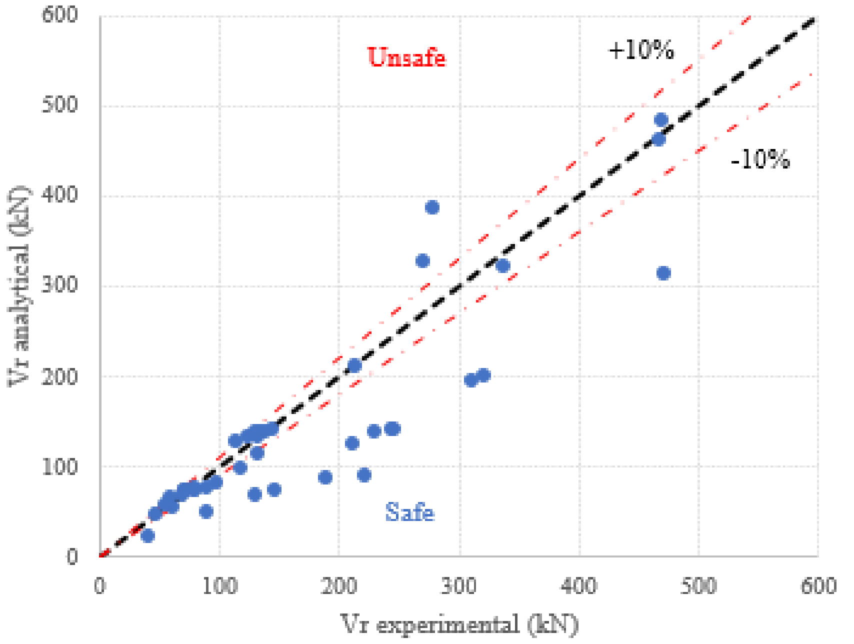

Figure 8. Residual shear force: analytical vs. experimental.

Analyzing the data in Table 5, it is possible to find an average ratio of $V_{r1}^{ana} / V_r^{exp} = 0.85$ and an average standard deviation of 0.23. The confidence interval was calculated with a 95% confidence level. A total of 47.5% of the beams are within the range V_{r1}^{ana} / V_r^{exp} of 0.90 and 1.10 and only two beams (5%) outside the adopted safety margin ($V_{r1}^{ana} / V_r^{exp} > 1.1$): the samples “test nº14” and “test nº18”.

The results showed to be more conservative for samples submitted to longer fire times (180min), however, due to the sudden and undesirable shear failure, it is prudent that the procedure has this premise. The analytical proposal, therefore, succeeds to estimate with reasonable precision and with safety the residual shear capacity of reinforced concrete beams after fire.

5 CONCLUSIONS

The study evaluated an analytical procedure for determining residual capacity for the bending moment and shear force of reinforced concrete beams after fire. The proposal was evaluated from experimental results of 62 reinforced concrete beams available in the literature. With the results, it is possible to conclude:

- The 500ºC isotherm method associated with the reduction coefficients presented here allows the assessment of residual strength to the bending moment with a correction factor of 1.2;
- The shear residual capacity to considering the influence of the ratio (a/d) applied to the 500ºC isotherm method and associated with the reduction coefficients presented here made it possible to predict shear capacity without the need for a correction factor;
- Shear capacity after fire can become the primary failure mode and needs to be considered in the analysis of strength after fire.

REFERENCES

[1] Y. Yang, S. Feng, Y. Xue, Y. Yu, H. Wang, and Y. Chen, "Experimental study on shear behavior of fire-damaged reinforced concrete T-beams retrofitted with prestressed steel straps," *Constr. Build. Mater.*, vol. 209, pp. 644–654, 2019, http://dx.doi.org/10.1016/j.conbuildmat.2019.03.054.

[2] J. Wróblewska and R. Kowalski, "Assessing concrete strength in fire-damaged structures," *Constr. Build. Mater.*, vol. 254, pp. 119122, 2020, http://dx.doi.org/10.1016/j.conbuildmat.2020.119122.

[3] M. Usman, M. Yaqub, M. Auzair, W. Khaliq, M. Noman, and A. Afaq, "Restorability of strength and stiffness of fire damaged concrete using various composite confinement techniques," *Constr. Build. Mater.*, vol. 272, pp. 121984, 2021, http://dx.doi.org/10.1016/j.conbuildmat.2020.121984.

[4] I. C. Neves, J. C. Rodrigues, and A. P. Loureiro, "Mechanical properties of reinforcing and prestressing steels after heating," *J. Mater. Civ. Eng.*, vol. 8, no. 4, pp. 189–194, 1996, http://dx.doi.org/10.1061/(ASCE)0899-1561(1996)8:4(189).

[5] R. Van Coile, R. Caspeele, and L. Taerwe, "Towards a reliability-based post-fire assessment method for concrete slabs incorporating information from inspection," *Struct. Concr.*, vol. 15, no. 3, pp. 395–407, 2014, http://dx.doi.org/10.1002/suco.201300084.

[6] T. Molkens, R. Van Coile, and T. Gernay, "Assessment of damage and residual load bearing capacity of a concrete slab after fire: Applied reliability-based methodology," *Eng. Struct.*, vol. 150, pp. 969–985, 2017, http://dx.doi.org/10.1016/j.engstruct.2017.07.078.

[7] D. P. Thanaraj, N. Anand, P. Arulraj, and K. Al-Jabri, "Investigation on structural and thermal performance of reinforced concrete beams exposed to standard fire," *J. Build. Eng.*, vol. 32, pp. 101764, 2020, http://dx.doi.org/10.1016/j.jobe.2020.101764.

[8] M. Diab, "Shear capacity of reinforced concrete beams at elevated temperatures," M.S. thesis, The Sch. Graduate and Postdoc. Stud., Western Univ.London, Ontario, Canada, 2014.

[9] Associação Brasileira de Normas Técnicas, *Projeto de Estruturas de Concreto em Situação de Incêndio*, NBR 15200, 2012.

[10] European Committee for Standardization, *Eurocode 1: Actions on Structures - Part 1-2: General Actions – Actions on Structures Exposed to Fire*, EN 1991-1-2, 2002.

[11] European Committee for Standardization, *Eurocode 2: Design of Concrete Structures - Part 1-2: General Rules – Structural Fire Design*, EN 1992-1-2, 2004.

[12] M. S. Cülfik and T. Özturan, "Effect of elevated temperatures on the residual mechanical properties of high-performance mortar," *Cement Concr. Res.*, vol. 32, no. 5, pp. 809–816, 2002, http://dx.doi.org/10.1016/S0008-8846(02)00709-3.

[13] F. Sciarretta, "Modeling of mechanical damage in traditional brickwork walls after fire exposure," *Adv. Mat. Res.*, vol. 919-921, pp. 495–499, 2014, http://dx.doi.org/10.4028/www.scientific.net/AMR.919-921.495.

[14] J. H. Hsu and C. S. Lin, "Effect of fire on the residual mechanical properties and structural performance of reinforced concrete beams," *J. Fire Prot. Eng.*, vol. 18, no. 4, pp. 245–274, Nov 2008, http://dx.doi.org/10.1177/1042391507077171.

[15] American Concrete Institute. *Building Code Requirements for Structural Concrete and Commentary*, ACI 318R-02, 2002.

[16] V. K. R. Kodur, M. B. Dwaikat, and R. S. Fike, "An approach for evaluating the residual strength of fire-exposed RC beams," *Mag. Concr. Res.*, vol. 62, no. 7, pp. 479–488, 2010, http://dx.doi.org/10.1680/macr.2010.62.7.479.

[17] American Concrete Institute, *Building Code Requirements for Reinforced Concrete*, ACI 318-08, 2008.

[18] L. Bai and Z. Wang, "Residual bearing capacity of reinforced concrete member after exposure to high temperature," *Adv. Mat. Res.*, vol. 368, no. 373, pp. 577–581, Oct 2011, http://dx.doi.org/10.4028/www.scientific.net/AMR.368-373.577.

[19] Y. Xu, B. Wu, M. Jiang, and X. Huang, "Experimental study on residual flexural behavior of reinforced concrete beams after exposure to fire," *Adv. Mat. Res.*, vol. 457-458, pp. 183–187, Jan 2012. [Online]. Available: 10.4028/www.scientific.net/AMR.457-458.183

[20] Y. Xu, B. Wu, R. Wang, M. Jiang, and Y. Luo, "Experimental study on residual performance of reinforced concrete beams after fire," *J. Build. Struct.*, vol. 34, no. 8, 2013.

[21] Y. Xu, X. Peng, Y. Dong, Y. Luo, and B. Lin, "Experimental study on shear behavior of reinforced concrete beams strengthened with CFRP sheet after fire," *J. Build. Struct. China*, vol. 36, no. 2, 2015. http://dx.doi.org/10.14006/j.jzjgxb.2015.02.015.

[22] GB, *Code for Design of Concrete Structures*, GB 50010, 2010.

[23] V. K. R. Kodur and A. Agrawal, "An approach for evaluating residual capacity of reinforced concrete beams exposed to fire," *Eng. Struct.*, vol. 110, pp. 293–306, Nov 2016, http://dx.doi.org/10.1016/j.engstruct.2015.11.047.

[24] R. Sun, B. Xie, R. Perera, and Y. Pan, "Modeling of reinforced concrete beams exposed to fire by using a spectral approach," *Adv. Mater. Sci. Eng.*, vol. 2018, pp. 1–12, 2018, http://dx.doi.org/10.1155/2018/6936371.

[25] B. Cai, L.-F. Xu, and F. Fu, "Shear resistance prediction of post-fire reinforced concrete beams using artificial neural network," *Int. J. Concr. Struct. Mater.*, vol. 13, no. 1, pp. 46, 2019, http://dx.doi.org/10.1186/s40069-019-0358-8.

[26] R. G. Pereira, T. A. C. Pires, D. C. L. Duarte, and J. J. R. Silva, "Assess of residual mechanical resistance of reinforced concrete beams after fire," *Rev. ALCONPAT*, vol. 9, no. 1, 2018, http://dx.doi.org/10.21041/ra.v9i1.299.

[27] A. Kumar and V. Kumar, "Behaviour of RCC beams after exposure to elevated temperatures," *J. Inst. Eng.*, vol. 84, pp. 165–170, 2003.

[28] Y. Song et al., "Residual shear capacity of reinforced concrete beams after fire exposure," *KSCE J. Civ. Eng.*, vol. 24, no. 11, pp. 3330–3341, 2020, http://dx.doi.org/10.1007/s12205-020-1758-7.

[29] H. Nakamura, T. Iwamoto, L. Fu, Y. Yamamoto, T. Miura, and Y. H. Gedik, "Shear resistance mechanism evaluation of RC beams based on arch and beam actions," *J. Adv. Concr. Technol.*, vol. 16, no. 11, pp. 563–576, Nov 2018, http://dx.doi.org/10.3151/jact.16.563.

[30] G. R. Plasencia, J. D. B. Rocha, J. J. H. Santana, and L. Pudipedi, "Study of the behavior of reinforced concrete deep beams: estimate of the ultime shear capacity," *Rev. Constr.*, vol. 16, no. 1, 2017. http://dx.doi.org/10.7764/RDLC.16.1.43.

[31] R. Kowalski and P. Król, "Experimental examination of residual load bearing capacity of RC beams heated up to high temperature," in *Proc. 6th Int. Conf. Struct. Fire*, East Lansing, Michigan, USA, 2010, pp. 254–261

[32] M. Głowacki and R. Kowalski, "An experimental approach to the estimation of stiffness changes in RC elements exposed to bending and high temperature," *Eng. Struct.*, vol. 217, pp. 110720, 2020., http://dx.doi.org/10.1016/j.engstruct.2020.110720.

[33] European Committee for Standardization, *Eurocode 2 – Design of Concrete Structures – Part 1-2: General Rules – Structural Fire Design*, EN 1992-1-1, 2004.

[34] K. Xiang, G. Wang, and H. Liu, "Shear strength of reinforced concrete beams after fire," *Appl. Mech. Mater.*, vol. 256-259, pp. 742–748, Dec 2012, http://dx.doi.org/10.4028/www.scientific.net/AMM.256-259.742.

[35] Associação Brasileira de Normas Técnicas, *Projeto de Estruturas de Concreto – Procedimento*, NBR 6118, 2014.

[36] T. Hayashikawa, F. Saido, and I. Higai, "Strength of RC deep beams with shear reinforcement," *Proc. Jpn. Concr. Inst.*, vol. 12, no. 2, pp. 319–324, 1990. In Japanese.

[37] M. R. F. Coelho, J. M. Sena-Cruz, and L. A. C. Neves, "Review on the bond behavior of FRP NSM systems in concrete," *Constr. Build. Mater.*, vol. 93, pp. 1157–1169, Sep 2015., http://dx.doi.org/10.1016/j.conbuildmat.2015.05.010.

Author contributions: LMC: conceptualization, methodology, bibliographic research, data analysis; JJRS: conceptualization, methodology, drafting, supervision; TACP: conceptualization, supervision, drafting and formal analysis, DCLD: writing and formal analysis.

Editors: Fernando S. Fonseca, Guilherme Aris Parsekian.